

Original Article

Long noncoding RNA TOB1-AS1, an epigenetically silenced gene, functioned as a novel tumor suppressor by sponging miR-27b in cervical cancer

Jihang Yao¹, Zhenghong Li¹, Ziwei Yang², Hui Xue¹, Hua Chang¹, Xue Zhang¹, Tianren Li¹, Kejun Guo¹

Departments of ¹Gynecology, ²Clinical Laboratory, The First Hospital of China Medical University, Shenyang 110001, Liaoning, China

Received April 21, 2018; Accepted July 9, 2018; Epub August 1, 2018; Published August 15, 2018

Abstract: Cervical cancer is one of the most common cancers in females, accounting for a majority of cancer-related deaths in worldwide. Long non-coding RNAs (lncRNAs) have been identified as critical regulators in many tumor-related biological processes. Thus, investigation into the function and mechanism of lncRNAs in the development of cervical cancer is very necessary. In this study, we found that the expression of TOB1-AS1 was significantly decreased in cervical cancer tissues compared with the adjacent normal tissues. The methylation status of TOB1-AS1-related CpG island was analyzed using methylation specific PCR and bisulfite sequencing analysis, revealing that the aberrant hypermethylation of TOB1-AS1-related CpG island was frequently observed in primary tumors and cervical cancer cells. The expression of TOB1-AS1 in cervical cancer cells could be reversed by demethylation agent treatment. Functionally, overexpression of TOB1-AS1 significantly inhibited cell proliferation, cell cycle progression, invasion and induced apoptosis, while knockdown of TOB1-AS1 exhibited the opposite effect. Furthermore, it was determined that TOB1-AS1 was able to bind and degrade the expression of miR-27b. Upregulation of miR-27b promoted cell growth, cell cycle transition from G1 phase to S phase, and invasion and reduced apoptosis, phenomenon could be reversed by TOB1-AS1. Inhibition of miR-27b attenuated the promotive effect of si-TOB1-AS1 on cellular processes. Upregulation of TOB1-AS1 also suppressed tumor growth *in vivo*. Clinically, methylation of TOB1-AS1 and low expression of TOB1-AS1 was significantly correlated with tumor stage and tumor size, respectively. Univariate and multivariate analyses confirmed that low level of TOB1-AS1 was an independent risk factor for death. In conclusion, we suggested that the epigenetically silenced TOB1-AS1 was unable to restrain miR-27b, which contributed to cervical cancer progression.

Keywords: TOB1-AS1, methylation, miR-27b, proliferation, apoptosis, invasion, cervical cancer

Introduction

Cervical cancer is the second leading cause of cancer-related death in women worldwide, with an estimated incidence of 500,000 cases and approximately 233,000 deaths per year [1, 2]. Cervical cancer is a multi-step process involving the deregulation of multiple genes; therefore, studies on the potential mechanisms underlying the initiation and progression of cervical cancer are absolutely necessary.

It is well known that 98% of DNA sequence in human genome may be transcribed to non-coding RNAs (ncRNAs) that lack the capacity to encode proteins [3]. Long non-coding RNAs (lnc-

RNAs), a group of ncRNAs (more than 200 nucleotides), have attracting more and more attentions in the field of cancer biology. Increasing studies has revealed a close relation between lncRNAs and human malignancy [4, 5]. Several lncRNAs have been verified to be associated with various tumor related processes, such as proliferation, apoptosis, migration, and invasion [6, 7]. For example, PVT1 was upregulated in cervical cancer cells and knockdown of PVT1 led to an inhibition of cell viability and motility [8]. Overexpression of HOXA11-AS contributed to cell proliferation, migration, and invasion *in vitro*, while silencing of HOXA11-AS exhibited the opposite effect on cellular processes [9]. Additionally, many differentially

expressed lncRNAs, such as MEG3 and MALAT1, have potential application in clinical diagnosis and prognosis for cancer patients [10, 11].

MicroRNAs (miRNAs) are a class of ncRNAs with a length of 18-22 nucleotides that have been reported to be oncogenes or tumor suppressors [12]. Accumulating studies have reported that lncRNAs may exert their roles in carcinogenesis by competitively binding to tumor-related miRNAs [13, 14]. For example, MEG3 decreased the expression level of miR-21-5p, followed by inducing cell growth inhibition and apoptosis in cervical cancer cells [15]. CCAT1 antagonized the effect of miR-410, which could promote cell proliferation and reduce apoptosis by suppressing ITPKB expression in colon cancer [16]. HOTAIR knockdown led to the inhibition of migration and invasion via decreasing of miR-206 in cervical cancer cells [17].

Human transducer of ERBB2.1 (TOB1), a member of the TOB/BTG family, was reported as an anti-proliferative protein in various cancers. Decreased expression of TOB1 has been observed in many cancers including breast, lung, and skin carcinoma [18-20]. Besides, upregulation of TOB1 promoted cell migration and invasion and induced apoptosis in gastric cancer cells [21, 22]. TOB1 antisense RNA 1 (TOB1-AS1), a novel lncRNA, is originated from the TOB1 gene cluster located on chromosome 17q21.33 in an antisense manner. However, the function and molecular mechanism of TOB1-AS1 have not been investigated. In this study, we focused on the function and mechanism of TOB1-AS1 in the development of cervical cancer.

Materials and methods

Clinical samples and cells

Cervical cancer tissues (n=50) and adjacent non-tumor tissues (n=50) were obtained from patients who were diagnosed at the Department of Gynecology, the First Hospital of China Medical University between Feb 2011 and Dec 2012. This study was approved by the Ethics Approval Committee of the First Hospital of China Medical University and all written informed consents were signed by patients. None of the patients had received chemo- or radio-

therapy before surgery. The histological type and tumor stage were identified according to the International Federation of Gynecology and Obstetrics (FIGO) classification system. All the tissue samples were snap-frozen in liquid nitrogen immediately following surgical resection, and stored in -80°C until use.

The human cervical cancer cell lines (SiHa, HeLa, CaSki, and C33A) human immortalized keratinocytes (HaCaT) cells were purchased from the Cell Bank of the Chinese Academy of Sciences (Shanghai, China) and cultured in DMEM (Gibco, Waltham, MA, USA) medium supplemented with 10% fetal bovine serum (FBS, Gibco), 100 g/ml streptomycin sulfate and 100 U/ml penicillin sodium. All cells were maintained at 37°C in a humidified atmosphere with 5% CO₂.

Plasmid construction and oligonucleotide transfection

Small interfering RNA (siRNA) and non-specific control siRNA (si-ctrl) were synthesized by GenePharma Co., Ltd. (Shanghai, China) and transfected into cells by using Lipofectamine 3000 (Invitrogen, Carlsbad, CA, USA). The sequences of si-TOB1-AS1 were as follows: si-RNA1, 5'-GCACCCGATTAATTGAATA-3'; si-RNA2, 5'-GC-GACTCGGATCCGTTTAT-3'. To construct TOB1-AS1 overexpression plasmid, the complementary DNA of TOB1-AS1 was amplified and cloned into pcDNA3.1 vector (Invitrogen) and named as pcTOB1-AS1. The empty vector was used as the negative control (pcDNA3.1). MiR-27b mimic, miR-27b inhibitor, mimic negative control (mim con), and inhibitor negative control (inh con) were synthesized by GenePharma Co., Ltd. (Shanghai, China). The miRNAs, siRNAs or plasmids were transfected/co-transfected by using Lipofectamine 3000 reagent (Invitrogen) according to the manufacturer's instructions. At 48 h after transfection/co-transfection, cells were subjected to further experimentation.

Quantitative real-time PCR (qRT-PCR)

Total RNA was extracted from cells and tissues using TRIzol reagent (Invitrogen). The PrimeScript™ Reverse Transcription Kit (TakaRa, Japan) was used to generate complementary DNA using in an ABI 7500 System (ABI, Foster City, CA, USA). MiRNA was isolated using the mir-Vana miRNA Isolation Kit (Ambion, Austin,

TOB1-AS1/miR-27b axis regulates cervical cancer progression

TX, USA) and cDNA was synthesized using the SuperScript II Reverse kit (Invitrogen). The SYBR Green Real-time PCR Master Mix (Takara) was used in qRT-PCR reaction and the quantitative data was calculated using the $2^{-\Delta\Delta Ct}$ method. GAPDH and U6 were used as internal control. Primers were as follows: TOB1-AS1, 5'-GC-CAGGCCTAGAAGCTTTT-3' (forward), 5'-TCTT-CCCACCCCTTCTCCTA-3' (reverse); GAPDH, 5'-CGACTTATACATGGCCTTA-3' (forward), 5'-TTCC-GATCACTGTTGGAAT-3' (reverse); U6, 5'-CTCG-CTTCGGCAGCAC-3' (forward), 5'-AACGCTTCA-CGAATTTGCGT-3' (reverse). All samples were run in triplicates.

Methylation specific PCR (MSP) and bisulphite sequencing analysis

DNA was isolated from cells and tissues using DNeasy Blood & Tissue Kit (Qiagen, Düsseldorf, Germany) and then subjected to bisulfite treatment using the EpiTect Bisulfite kit (Qiagen). For MSP assay, the primer pairs for both the methylated and unmethylated sequences was used in cells, while in tissues only methylated sequences was used. The MSP reaction was performed using a Technet-512 (Technet, Staffordshire, UK). Primer sequences were as follows: methylated, 5'-AAGGGAGGTCGTTATAGTTTC-3' (forward) and 5'-CATACGCAATTAACCTCGT-3' (reverse); unmethylated, 5'-GAAGGGAGGTTGTTATAGTT-3' (forward) and 5'-TACATACACAATTAACCTCATA-3' (reverse). The products were visualized on 2% agarose gels.

The fragment containing the TOB1-AS1-related CpG island was analyzed using Methyl Primers Express software (ABI) to identify primers which used for bisulfite sequencing. These primers (forward: 5'-GGTAGAGAAAGGGTAAATTGTGAT-3' and reverse: 5'-ATCCAACAAACCCTAAAAATAC-3') were used to amplify bisulphite-converted DNA of the target region (356 bp) containing 23 CpG sites. The PCR product was cloned into the pCR4 vector (Invitrogen) and 5 positive clones were selected for sequencing analysis. The methylation result was analyzed using BiQ Analyzer software to generate a lollipop diagram.

5-aza-2-deoxycytidine treatment

The demethylation treatment was performed with four different concentrations (0, 5, 10 and

20 μ M) of 5-aza-2-deoxycytidine (5-aza) (Sigma, St. Louis, MO, USA). The fresh medium containing 5-aza was changed every 24 h for 3 days and cells were obtained at 72 h.

Cell proliferation assay

A total of 2×10^3 cells (per well) were seeded in 96-well plates in triplicate. At 24, 48, 72, and 96 h after transfection, the cells were incubated with MTT (5 mg/mL; Sigma) for 4 h at 37°C. DMSO was added to each well to stop the reaction and the optical density (OD) of each well was measured at 490 nm using a microplate reader (Bio-Rad, Hercules, CA, USA).

Cell cycle distribution and apoptosis analysis

The transfected cells were trypsinized, washed, fixed with ice-cold 70% ethanol, and stored at 4°C overnight. Then, the cells were washed with PBS and stained with propidium iodide (PI, Sigma)/RNAase for 30 min at room temperature. Cell cycle distribution was detected and analyzed using the FACSCalibur flow cytometry (BD Biosciences, San Jose, CA, USA) and ModFit software (Verity Software, Topsham, ME, USA).

Apoptosis assay was performed using Annexin V-FITC/PI Apoptosis Detection Kit (Vazyme, Nanjing, China). Cells were washed, resuspended in binding buffer and 5 μ l of PI and 5 μ l Annexin V-FITC were added to the cell suspension and incubated for 15 min in the dark. Cell samples were analyzed with a FACSCalibur flow cytometry (BD Biosciences).

Transwell invasion assay

The invasive ability of cells were detected using a Transwell chamber with a layer of Matrigel (Millipore, Billerica, MA, USA). Briefly, cells (2×10^5 per well) were seeded into the upper chamber filled with serum-free medium. The lower chamber was filled with medium with 10% FBS. After incubation at 37°C for 24 h, cells adhered on the upper surface of the membrane were removed, while the cells invaded into the lower chamber were fixed in methanol and stained with 0.1% crystal violet (Sigma) for 15 min at 37°C. For each well, five random fields were counted and the average number of cells was determined under a light microscope.

TOB1-AS1/miR-27b axis regulates cervical cancer progression

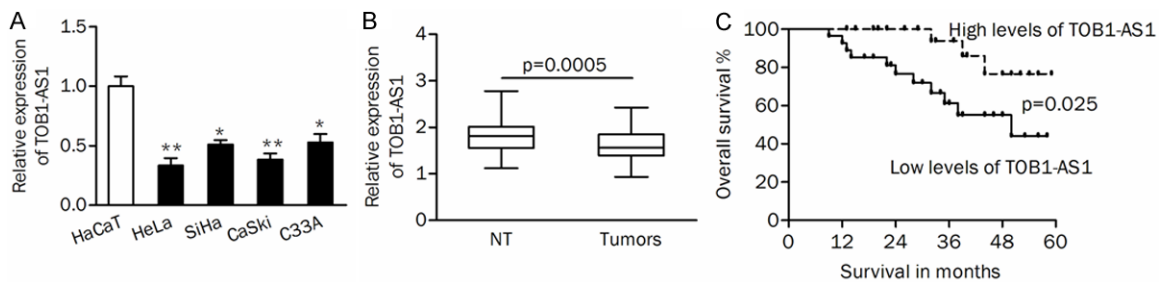


Figure 1. TOB1-AS1 was downregulated in cervical cancer tissues. A. QRT-PCR was used to determine the endogenous levels of TOB1-AS1 in cervical cancer cells and normal control HaCaT cells. B. The expression of TOB1-AS1 was significantly decreased in primary tumors. C. High expression of TOB1-AS1 indicated a better prognosis of patients. NT, non-tumor tissues; * $P < 0.05$; ** $P < 0.01$.

Reporter vectors construction and luciferase assays

We used the bioinformatics databases (Starbase v2.0) to search for potential miRNAs that can bind to TOB1-AS1. The fragment from TOB1-AS1 containing the predicted miR-27b binding site was amplified by PCR and cloned into a pmirGLO Dual-luciferase Target Expression Vector (Promega, Madison, WI, USA) to generate the wide type reporter vector (TOB1-AS1-WT). The mutant was created by mutating the miR-27b seed sequence, which were named as TOB1-AS1-Mut. HeLa cells were co-transfected with the pmirGLO vector with either wild type fragments (or mutation fragments) and miR-27b mimic (or mimic control) using Lipofectamine 3000. The mutant without miR-27b binding site were also used as negative control and named as pmirGLO. 48 h later, luciferase reporter assay was performed using the Dual-Luciferase Reporter Assay System (Promega).

RNA in situ hybridization

Cy3-labeled TOB1-AS1 probes and Dig-labeled locked nucleic acid miR-27b probes were designed and synthesized by RiboBio (Guangzhou, China). The signals of the probes were tested by Fluorescent In Situ Hybridization Kit (RiboBio, Guangzhou, China) according to the manufacturer's instructions and the images were obtained using Nikon A1Si Laser Scanning Confocal Microscope (Nikon, Japan).

Western blotting assay

Cells were lysed using ice-cold RIPA buffer (Beyotime, Shanghai, China) for 30 min and

protein concentration was analyzed by the BCA protein assay kit (Thermo, Waltham, MA, USA). Equal amounts of protein (20 μ g) were separated on 10% SDS-PAGE gel and transferred to the polyvinylidene difluoride (PVDF) membranes (Thermo). The membranes were blocked with 5% non-fat milk for 1 h at room temperature, and then incubated with the primary antibody against Cyclin D1 (1:1,000, ab134175; Abcam, Cambridge, MA, USA), Bax (1:1,000, ab325-03), E-cadherin (1:1,000, ab1416), N-cadherin (1:1,000, ab76011), and β -actin (1:1,000, ab8-226) at 4°C overnight. Membranes were then washed three times and incubated with goat anti-mouse (ab205719) or goat anti-rabbit (ab205718) horseradish peroxidase conjugated secondary antibody for 2 h at room temperature. The blots were visualized using enhanced chemiluminescence (ECL) kit (Santa Cruz Bio., Santa Cruz, CA, USA).

Xenograft model

This study was performed in accordance with the Declaration of Helsinki and has been approved by the ethical committee of the First Hospital of China Medical University. Female BALB/c nude mice (4-5 weeks old) were randomly divided into two groups ($n=6$ for each group). A total of 5×10^6 HeLa cells transfected with pcTOB1-AS1 or pcDNA3.1 were collected and subcutaneously injected into the right flank of nude mice. Ten days later, size of tumor xenografts was estimated for every 5 days using a caliper and the tumor volume was calculated as follows: length \times width² \times 1/2. The mice were euthanized at the end of the study, and the tumor xenografts were obtained and weighed.

TOB1-AS1/miR-27b axis regulates cervical cancer progression

Table 1. Correlations between the dysregulated moleculars and clinicopathological features of patients

Features	No. Cases		Methylation status		P	Expression of TOB1-AS1		P
	n=50	Neg, n=32	Pos, n=18			High, n=23	Low, n=27	
Age (years)					0.273			0.673
<40	19	14	5			8	11	
≥40	31	18	13			15	16	
Tumor size					0.907			0.002
<4 cm	30	19	11			19	11	
≥4 cm	20	13	7			4	16	
Differentiation					0.020			0.952
Well+mod	35	26	9			16	19	
Poor	15	6	9			7	8	
FIGO stage					0.002			0.077
I	28	23	5			16	12	
II	22	9	13			7	15	
Vascular involvement					0.099			0.838
Negative	44	30	14			20	24	
Positive	6	2	4			3	3	
HPV16/18					0.647			0.736
Negative	38	25	13			18	20	
Positive	12	7	5			5	7	
Histology					0.569			0.535
SCC	41	27	14			18	23	
ADC	9	5	4			5	4	

mod, moderate; SCC, Squamous cell carcinoma; ADC, Adenocarcinoma.

Table 2. Characteristics of patients associate with survival of patients by Cox proportional hazard regression analysis

Features	Univariate			Multivariate		
	HRs	P	CI	HRs	P	CI
Age (<40/≥40 years)	1.590	0.411	0.527-4.800			
Tumor size (<4/≥4 cm)	1.820	0.266	0.633-5.230			
Diff (well+mod/poor)	2.637	0.071	0.921-7.552			
FIGO stage (I/II)	2.225	0.152	0.745-6.644			
Vascular involvement (neg/pos)	3.589	0.034	1.101-11.704	4.042	0.021	1.233-13.248
HPV16/18 (neg/pos)	0.963	0.953	0.268-3.457			
Histology (SCC/ADC)	1.406	0.568	0.437-4.523			
Methy-TOB1-AS1 (neg/pos)	1.875	0.241	0.656-5.365			
TOB1-AS1 (high/low)	3.874	0.038	1.079-13.915	4.182	0.029	1.159-15.088

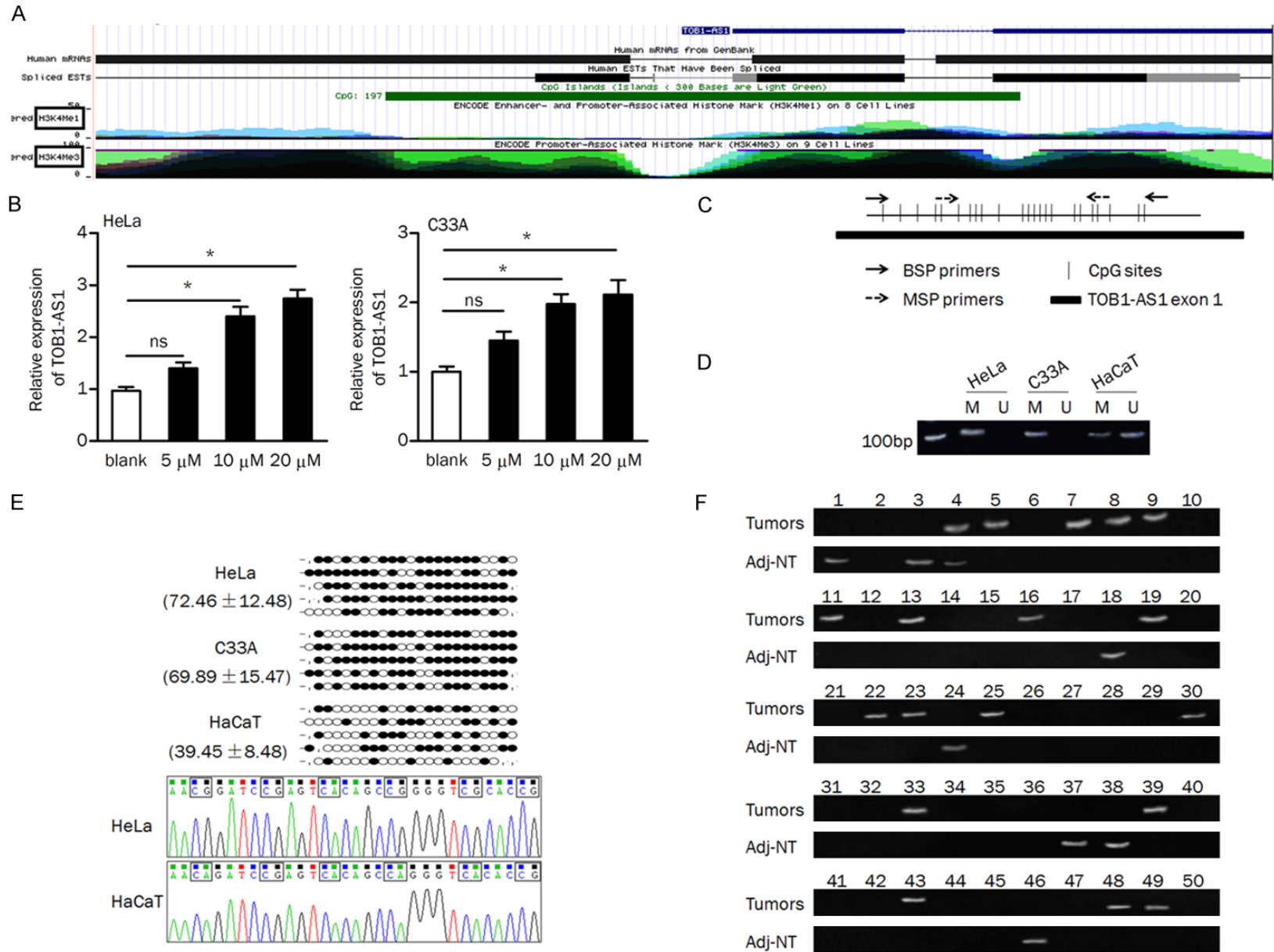
HRs, hazard ratios; CI, confidence intervals; Diff, differentiation; mod, moderate; neg, negative; pos, positive; SCC, squamous cell carcinoma; ADC, adenocarcinoma; Methy-TOB1-AS1, methylation of TOB1-AS1.

Statistical analysis

All values were expressed as mean ± standard deviation (SD) from at least three independent experiments and statistical analyses were performed using student's t-test with SPSS 16.0 (IBM, Armonk, NY, USA) software. Kaplan-Meier

method was used for analysis of overall survival of patients and Cox proportional hazards model was used for analysis of prognostic factors. GraphPad Prism 5.0 (GraphPad, La Jolla, CA, USA) software was used to generate graphs. P<0.05 was considered to be statistically significant.

TOB1-AS1/miR-27b axis regulates cervical cancer progression



TOB1-AS1/miR-27b axis regulates cervical cancer progression

Figure 2. DNA methylation regulated the expression of TOB1-AS1. A. Schema of the TOB1-AS1 location from the UCSC Genome Browser, Green block indicates the CpG island. B. HeLa and C33A cells were treated with 5-aza (0/5/10/20 μM) for three days and TOB1-AS1 expression was tested. C. Schema of the map of the TOB1-AS1-related CpG island and location of the primers; CpG sites are indicated with vertical ticks. D. The methylation status of TOB1-AS1 in cells was examined by MSP; M, methylated; U, unmethylated. E. Methylation status of the 23 CpG sites and representative sequences of bisulfite sequencing analysis in cells. Black dot, methylated CpG; white dot, unmethylated CpG; stub, not available. F. The methylation status of TOB1-AS1 in tumors and adjacent non-tumor tissues; methylated products were observed in 18 tumors and 8 normal tissues, respectively. ns, no significance; Adj-NT, adjacent nontumorous tissues. * $P < 0.05$.

Table 3. The methylated TOB1-AS1 was tested in tissue specimens

	Methylation		Total cases
	Positive	Non-positive	
Tumors	18	32	50
Normal tissues	8	42	50

Chi-Square test, $P = 0.023$

Results

TOB1-AS1 was downregulated in cervical cancer cells and tissues

The expression of TOB1-AS1 was detected in cervical cancer cells and tissues using qRT-PCR. As shown in **Figure 1A**, the results of qRT-PCR analysis showed that TOB1-AS1 was significantly downregulated in cervical cancer cells compared with control HaCaT cells. In addition, TOB1-AS1 expression was found to be significantly lower in cervical cancer tissues than that in adjacent non-tumor tissues (**Figure 1B**, $P = 0.0005$).

The correlations between the expression of TOB1-AS1 and clinicopathological characteristics of patients were shown in **Table 1**. The mean level of TOB1-AS1 in tumor tissues was used as cut-off to divide cases into two groups (low- or high-group). Low expression of TOB1-AS1 was significantly correlated with large tumor size ($P = 0.002$, **Table 1**). Kaplan-Meier analysis showed that high expression of TOB1-AS1 indicated a better overall survival for patients (**Figure 1C**, $P = 0.025$). Furthermore, univariate and multivariate analysis confirmed that vascular involvement ($P = 0.021$) and TOB1-AS1 low-expression ($P = 0.029$; **Table 2**) were independently associated with risk factors of death.

Epigenetically downregulated TOB1-AS1 in cervical cancer cells and tissues

More recently, several studies have revealed that DNA methylation was involved in mediating

the expression of lncRNAs in many cancers [23-25]. In here, we found that the first exon of TOB1-AS1 was embedded in a CpG island (**Figure 2A**). We intended to verify whether DNA methylation regulates the expression of TOB1-AS1. Firstly, we examined the effect of demethylation agent 5-aza on TOB1-AS1 expression. QRT-PCR analysis indicated that expression of TOB1-AS1 was significantly restored in the 5-aza (10 μM and 20 μM) treatment group compared to that in the control group (**Figure 2B**). The paired primers for MSP and bisulfite sequencing were designed to verify the methylation status of TOB1-AS1-related CpG island (**Figure 2C**). We found that the CpG island is totally methylated in HeLa and C33A cells, while partially methylated in HaCaT cells. The unmethylated product was observed in HaCaT cells but not in cervical cancer cells (**Figure 2D**). Furthermore, bisulfite sequencing data showed that the percentage of methylated CpG sites were obviously higher in cervical cancer cells than that in HaCaT cells (**Figure 2E**).

The methylation status of TOB1-AS1-related CpG island in primary cervical cancer tissues and nonmalignant tissues was measured by MSP. As shown in **Figure 2F**, the methylation of TOB1-AS1-related CpG island was more frequently observed in tumors than that in adjacent non-tumor tissues (36% vs. 16%, $P = 0.023$, **Table 3**). By spearman correlation coefficient analysis, we found that methylation of CpG island was significantly negative correlated with the expression of TOB1-AS1 in tumors (spearman's $r = -0.505$, $P < 0.01$, **Table 4**). Besides, we found that the methylation of TOB1-AS1-related CpG island was significantly associated with tumor differentiation ($P = 0.02$) and FIGO stage ($P = 0.002$, **Table 2**).

TOB1-AS1 inhibited cell proliferation, cell cycle progression, and invasion and induced apoptosis

To explore the function of TOB1-AS1 in cervical cancer cells, gain- and loss-of-function analyses were performed. In HeLa and C33A cells,

Table 4. The correlation between the methylation frequency of TOB1-AS1 and its expression levels

	Adj-NT	Tumors
Methylation frequency	16% (8/50)	36% (18/50)
Expression of TOB1-AS1	1.794±0.336	1.595±0.310
Spearman's r=-0.505, P<0.01		

qRT-PCR assays confirmed that TOB1-AS1 was significantly upregulated in HeLa cells after transfected with plasmid vector; and both si-RNA1 and si-RNA2 decreased the expression of TOB1-AS1 in C33A cells (**Figure 3A**).

The MTT assay revealed that ectopic expression of TOB1-AS1 significantly reduced cell proliferation rate; both si-RNA1 and si-RNA2 transfection promoted cell proliferation in C33A cells (**Figure 3B**). Flow cytometry analysis showed that introduction of TOB1-AS1 induced cell cycle arrest at G1 phase. Knockdown of TOB1-AS1 in C33A cells led to a significantly lower frequency of cells at G1 phase and a higher frequency of cells at S phase (**Figure 3C**). The percentage of apoptotic cells was increased by overexpression of TOB1-AS1 in HeLa cells, while decreased by knockdown of TOB1-AS1 in C33A cells (**Figure 3D**). Transwell invasion assay showed that cell invasion was markedly suppressed in HeLa cells transfected with pcTOB1-AS1. The cell invasive ability was increased in C33A cells after knocking down TOB1-AS1 (**Figure 3E**). These data indicated that TOB1-AS1 may function as a tumor suppressor by inhibiting cell growth, cell cycle progression, and invasion and promoting apoptosis.

Regulating relationship between TOB1-AS1 and miR-27b

The above data have revealed the tumor suppressor role of TOB1-AS1 and the possible mechanism responsible for its downregulation in cervical cancer progression. Considering that lncRNAs can function as miRNA sponges, bio-informatic tools was used to search for the potential miRNAs that can be regulated by TOB1-AS1. To our interest, miR-27b, which has been found to be upregulated in cervical cancer [26], was predicted as a target of TOB1-AS1 (**Figure 4A**). The result showed that miR-27b level was significantly decreased in HeLa/pcTOB1-AS1 cells than that in HeLa/pcDNA3.1 cells (**Figure 4B**). Knockdown of TOB1-AS1 by siRNA

(si-RNA1 and si-RNA2) transfection led to a significant increasing of miR-27b expression in C33A cells (**Figure 4C** and **4D**). In contrast, the expression of TOB1-AS1 was significantly decreased after miR-27b mimic transfection, while increased after miR-27b inhibitor transfection (**Figure 4E**). A luciferase activity assay was conducted and the results showed that co-transfection of miR-27b and TOB1-AS1-WT significantly reduced the luciferase activity (**Figure 4F**). Moreover, RNA FISH assay revealed that TOB1-AS1 and miR-27b were co-localized in cytoplasm (**Figure 4G**).

MiR-27b abrogates the effect of TOB1-AS1 on cell growth, apoptosis, and invasion

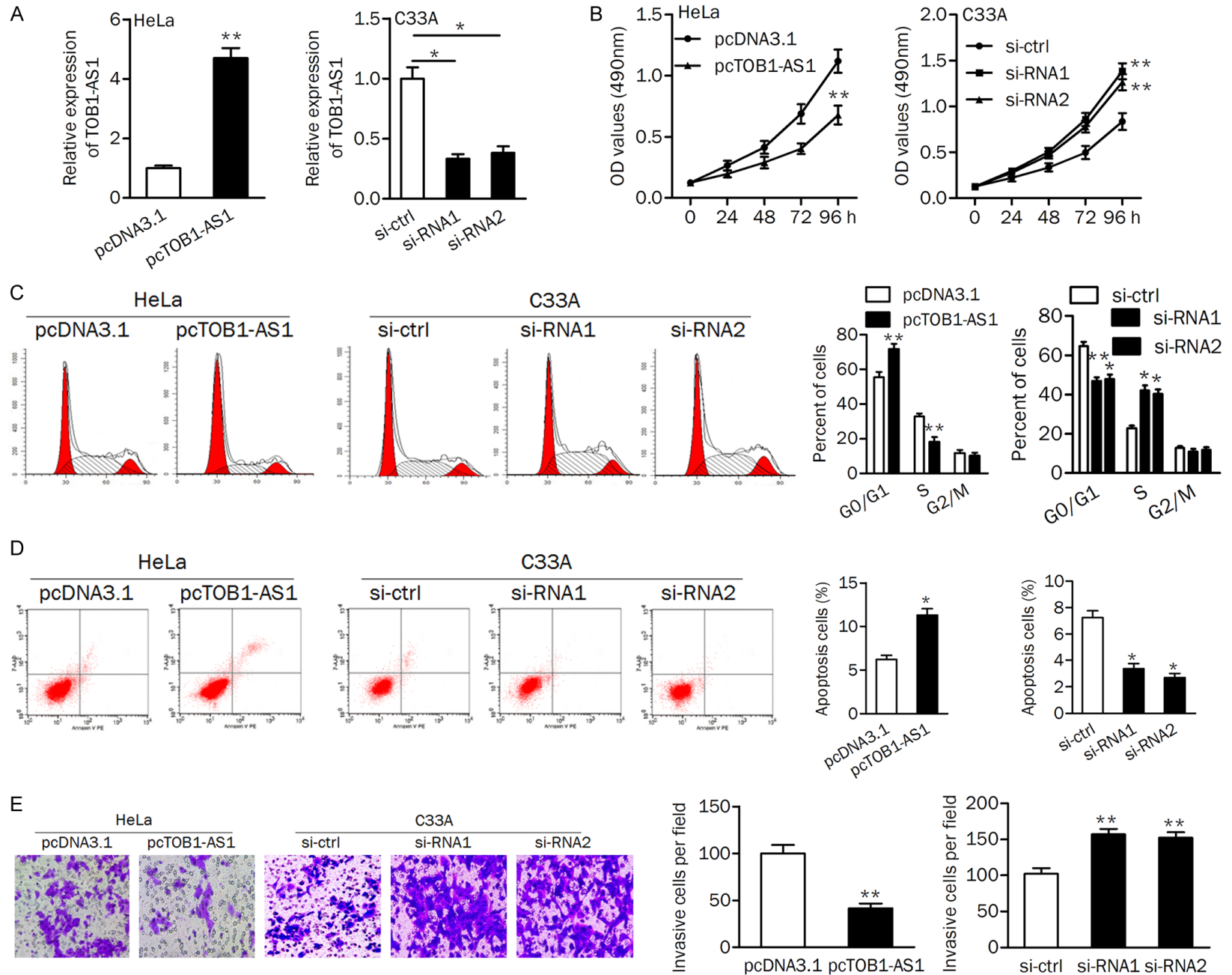
To explore the effect of miR-27b combined with TOB1-AS1 overexpression on cell viability and motility, HeLa cells were divided into four groups: transfected with mim con+pcDNA3.1, transfected with mimic+pcDNA3.1, transfected with mimic+pcTOB1-AS1, and transfected with mimic+pmirGLO. As shown in **Figure 5A**, ectopic of miR-27b promoted cell proliferation, phenomenon could be impaired by TOB1-AS1. Likewise, miR-27b mimic transfection induced cell cycle progression from G1 phase to S phase, which could be reversed by pcTOB1-AS1 (**Figure 5B**). Upregulation of TOB1-AS1 abolished the miR-27b induced inhibition of cell apoptosis (**Figure 5C**). TOB1-AS1 upregulation reversed the increasing of cell invasion induced by miR-27b (**Figure 5D**).

Furthermore, we verified the role of miR-27b inhibitor and TOB1-AS1 silencing in C33A cells. TOB1-AS1 inhibition abrogated the reducing of cell proliferation induced by si-RNA1 (**Figure 5E**). The percentage of cells at the S phase was significantly lower and the proportion of apoptotic cells was higher in cells transfected with miR-27b inhibitor+si-ctrl than that in cells transfected with miR-27b inhibitor+si-RNA1 (**Figure 5F** and **5G**). In addition, knockdown of TOB1-AS1 impaired the miR-27b inhibitor induced decreasing of cell invasion (**Figure 5H**).

TOB1-AS1 inhibits tumor growth in vivo

We detected the expression of G1/S phase checkpoint protein (cyclin D1), pro-apoptotic protein (Bax), and epithelial-mesenchymal tran-

TOB1-AS1/miR-27b axis regulates cervical cancer progression



TOB1-AS1/miR-27b axis regulates cervical cancer progression

Figure 3. TOB1-AS1 inhibited cell growth and invasion. A. PCR assay was used to verify the expression of TOB1-AS1 in cells. B. Overexpression of TOB1-AS1 in HeLa cells suppressed proliferation, while knockdown of TOB1-AS1 promoted proliferation of C33A cells. C. Upregulation of TOB1-AS1 induced cell cycle arrest at G1 phase; Silencing of TOB1-AS1 promoted cell cycle progression from G1 phase to S phase. D. Apoptotic cells were increased by pcTOB1-AS1 and decreased by si-RNA1 and si-RNA2. E. The invasion ability were assayed using the transwell assay in HeLa and C33A cells. pcDNA3.1, negative control; pcTOB1-AS1, TOB1-AS1 expressing plasmid; si-ctrl, siRNA control; si-RNA1/2, siRNAs for knocking down TOB1-AS1. *P<0.05; **P<0.01.

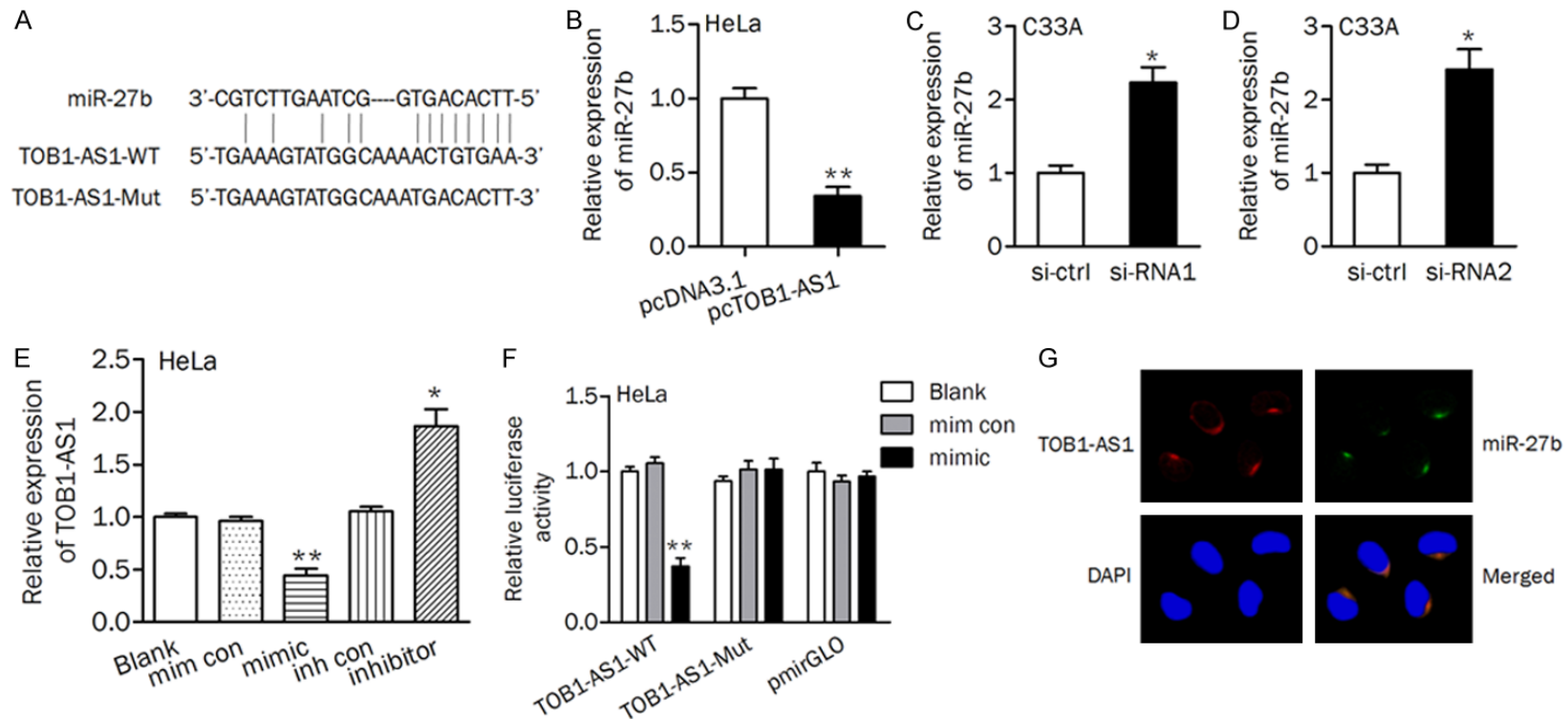
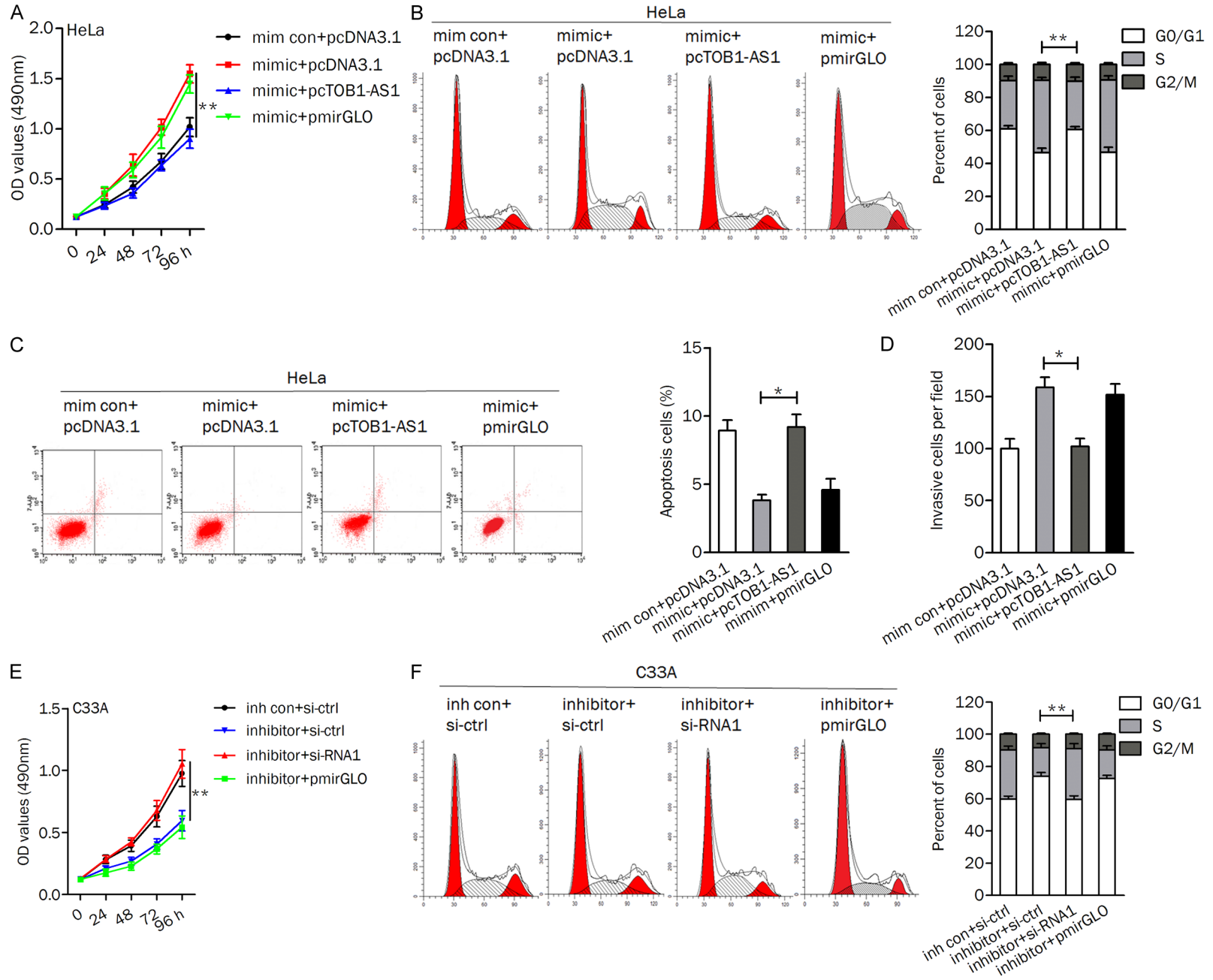


Figure 4. TOB1-AS1 sponged miR-27b with complementary binding at 3'-UTR. A. Schematic diagram showed the complementary bound within miR-27b and TOB1-AS1 3'-UTR with binding sites. B-D. The expression levels of miR-27b were tested after up- or downregulation of TOB1-AS1 in cervical cancer cells. E. The expression of TOB1-AS1 was evaluated. F. Luciferase reporter assay was performed in HeLa cells transfected with TOB1-AS1 wild (or mutant) type and miR-27b mimics (or mimic control). mim con, mimic control; inh con, inhibitor control. G. The co-localization between TOB1-AS1 and miR-27b in HeLa cells. *P<0.05; **P<0.01.

TOB1-AS1/miR-27b axis regulates cervical cancer progression



TOB1-AS1/miR-27b axis regulates cervical cancer progression

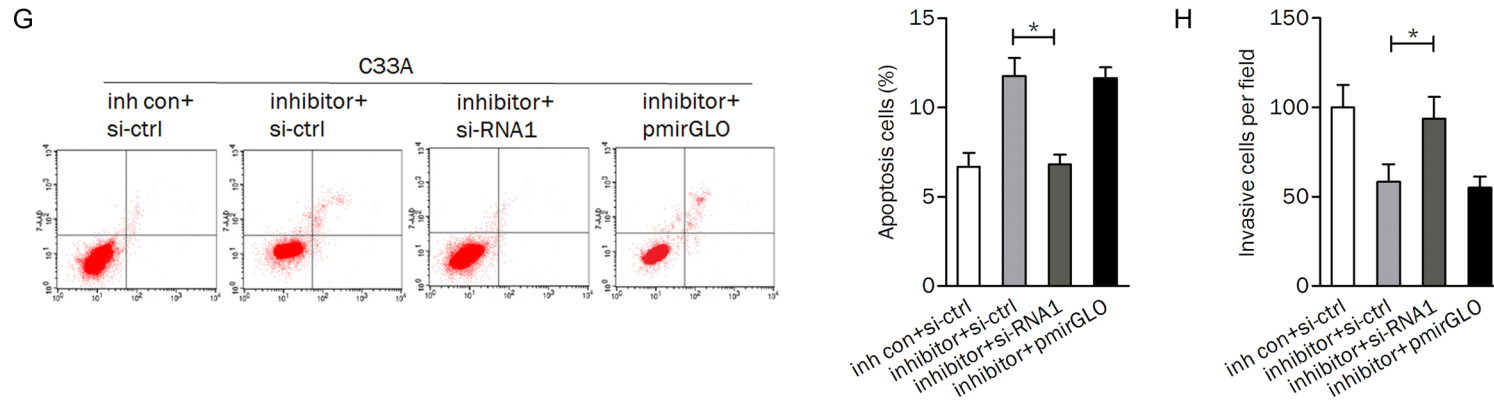


Figure 5. TOB1-AS1/miR-27b axis regulated cell viability and motility. (A-D) Overexpression of TOB1-AS1 reversed the miR-27b induced cell proliferation (A), cell cycle progression (B), apoptosis inhibition (C), and invasion (D) in HeLa cells. (E-H) Application of si-RNA1 attenuated the effect of miR-27b inhibitor exerted on cell growth (E), cell cycle distribution (F), apoptosis (G), and invasive ability (H). *P<0.05; **P<0.01.

TOB1-AS1/miR-27b axis regulates cervical cancer progression

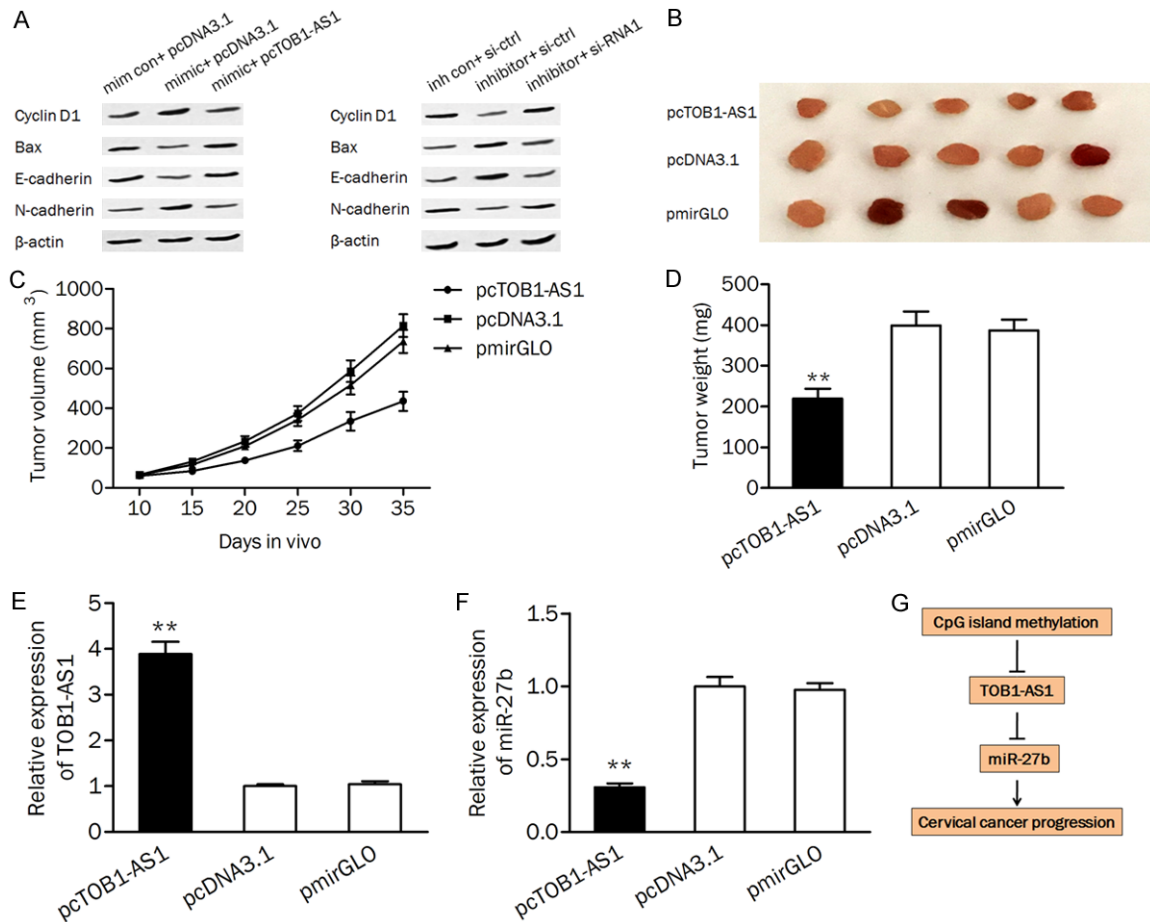


Figure 6. TOB1-AS1/miR-27b axis was involved in cell growth in vivo. (A) The protein levels of Cyclin D1, Bax, E-cadherin, and N-cadherin were detected by western blot analysis. (B) Representative xenograft tumors obtained from mouse injected with pcTOB1-AS1 or pcDNA3.1. (C and D) Construction of TOB1-AS1 stably expressing cells led to an decreasing of tumor volume (C) and weight (D). (E and F) The expression of TOB1-AS1 (E) and miR-27b (F) in xenograft tumors were measured by qPCR. (G) A schematic diagram deciphering the mechanism underlying the effect of epigenetically silenced TOB1-AS1 on the expression of miR-27b and cervical cancer progression. mim con, mimic control; inh con, inhibitor control. pcTOB1-AS1, TOB1-AS1 expressing plasmid; si-ctrl, siRNA control; si-RNA1, siRNA for knocking down TOB1-AS1; **P<0.01.

sitions (EMT) associated proteins (E-cadherin and N-cadherin) in cells. As shown in **Figure 6A**, application of miR-27b mimic increased the protein expression of cyclin D1, and N-cadherin and decreased the protein level of Bax and E-cadherin, phenomenon could be reversed by overexpression of TOB1-AS1. On the contrary, Knockdown of TOB1-AS1 abolished the miR-27b inhibitor induced the upregulating of Bax, and E-cadherin and the downregulation of cyclin D1, and N-cadherin.

To verify the effect of TOB1-AS1 on tumor growth in vivo, nude mice were subcutaneously inoculated with HeLa cells transfected with pcTOB1-AS1, pcDNA3.1, and pmirGLO, respec-

tively. As shown in **Figure 6B** and **6C**, overexpression of TOB1-AS1 significantly reduced the tumor volume in mouse. The tumor weight was also markedly decreased in the pcTOBA-AS1 treated group compared to the control group (**Figure 6D**). Furthermore, qRT-PCR analysis confirmed the significantly upregulated TOB1-AS1 and downregulated miR-27b in mouse transfected with pcTOB1-AS1 (**Figure 6E** and **6F**).

Discussion

Increasing number of lncRNAs have been identified as regulators and associated with the progression of cervical cancer, including HOTAIR,

MALAT1, and PVT1 [8, 27, 28]. In this study, we noted that a novel lncRNA TOB1-AS1 was down-regulated in cervical cancer cells and tissues and associated with poor prognosis of patients. Besides, the low expression of TOB1-AS1 was associated with the larger tumor size. Therefore, the abnormal of TOB1-AS1 may have a role in the development of cervical cancer.

It is well known that DNA methylation plays an important role in regulating tumor-related genes and miRNAs. Moreover, CpG island methylation could regulate the expression of lncRNAs such as MEG3, SOX21-AS1, and CRNDE [24, 25, 29]. Our data showed that TOB1-AS1 expression was increased in cervical cancer cells after treated with 5-aza. Bisulfite sequencing analysis also confirmed that TOB1-AS1-related CpG island were hypermethylated in cervical cancer cells. More importantly, methylation of CpG island was frequently observed in tumors and negatively correlated with the expression level of TOB1-AS1, suggesting that methylation of TOB1-AS1 at least partially resulted in its downregulation in the progression of cervical cancer. The methylation status of TOB1-AS1 was also correlated with differentiation and clinical stage of tumors, indicating that epigenetic modification of TOB1-AS1 might involved in cervical carcinogenesis.

MiR-27b is known to have important roles in many tumor-related processes, including proliferation, apoptosis, migration, invasion, and drug resistance [30-32]. Our previous study has revealed that miR-27b acted as an oncogene in cervical cancer by targeting CDH11 [26]. Increasing studies showed that lncRNAs can act as molecular sponges to competitively inhibit miRNAs. For example, HOXD4-AS1 exerts oncogenic functions through sponging miR-608 in ovarian cancer [33]. GAS5 can function as a competing endogenous RNA (ceRNA) for miR-21 [34]. TCONS_00026907 functions as a sponge of miR-143 to regulate cervical cancer progression [35]. We speculated that TOB1-AS1 might be a ceRNA in cervical cancer. Further experiments demonstrated the interaction between TOB1-AS1 and miR-27b. These data suggested that an inverse correlation may be existed between TOB1-AS1 and miR-27b. Besides, a luciferase activity assay confirmed the direct binding relationship between TOB1-AS1 and miR-27b. Recent studies demonstrated that UCA1 and ZEB2-AS1 function as a

ceRNA for miR-27b in different types of cancers [36, 37]. This implying that miR-27b may interact with various lncRNAs in different tumors.

Functionally, our data demonstrated that silencing of TOB1-AS1 using two independent siRNAs both significantly promoted proliferation, cell cycle progression, and invasion and induced apoptosis of C33A cells. Overexpression of TOB1-AS1 leads to inhibition of cell viability, and motility in vitro and tumor growth in vivo, indicating the tumor suppressive role of TOB1-AS1 in tumorigenesis. Furthermore, the inhibitory effect of TOB1-AS1 on biological processes could be attenuated by upregulation of miR-27b. The protein levels of Cyclin D1, Bax, E-cadherin, and N-cadherin were also regulated by TOB1-AS1 and miR-27b in cancer cells. These results supported the regulatroy effect of TOB1-AS1/miR-27b axis on cell proliferation, apoptosis, and invasion.

Taken together, low expression of TOB1-AS1 can serve as an independent biomarker for poor prognosis of cervical cancer patients. DNA hypermethylation might be at least partially responsible for the downregulation of TOB1-AS1, which failed to suppress the oncogenic role of miR-27b. We highlighted that TOB1-AS1 was downregulated in cervical cancer and acted as tumor suppressor through sponging miR-27b, and may provide a potential therapeutic target for cervical cancer treatment.

Acknowledgements

This research was supported by grants from the General Scientific Research Project of Universities in Liaoning (No. L2014139).

Disclosure of conflict of interest

None.

Address correspondence to: Kejun Guo, Department of Gynecology, The First Hospital of China Medical University, 155 Nanjingbei Street, Heping District, Shenyang 110001, Liaoning, China. Tel: +86-02483283516; E-mail: kejun_guo@hotmail.com

References

- [1] Parkin DM, Bray F, Ferlay J, Pisani P. Estimating the world cancer burden: Globocan 2000. *Int J Cancer* 2001; 94: 153-156.

TOB1-AS1/miR-27b axis regulates cervical cancer progression

- [2] Ellenson LH, Wu TC. Focus on endometrial and cervical cancer. *Cancer Cell* 2004; 5: 533-538.
- [3] Cheetham SW, Gruhl F, Mattick JS, Dinger ME. Long noncoding RNAs and the genetics of cancer. *Br J Cancer* 2013; 108: 2419-2425.
- [4] Schmitz SU, Grote P, Herrmann BG. Mechanisms of long noncoding RNA function in development and disease. *Cell Mol Life Sci* 2016; 73: 2491-2509.
- [5] Zhao M, Qiu Y, Yang B, Sun L, Hei K, Du X, Li Y. Long non-coding RNAs involved in gynecological cancer. *Int J Gynecol Cancer* 2014; 24: 1140-1145.
- [6] Guo X, Hua Y. CCAT1: an oncogenic long non-coding RNA in human cancers. *J Cancer Res Clin Oncol* 2017; 143: 555-562.
- [7] Lee NK, Lee JH, Ivan C, Ling H, Zhang X, Park CH, Calin GA, Lee SK. MALAT1 promoted invasiveness of gastric adenocarcinoma. *BMC Cancer* 2017; 17: 46.
- [8] Iden M, Fye S, Li K, Chowdhury T, Ramchandran R, Rader JS. The lncRNA PVT1 contributes to the cervical cancer phenotype and associates with poor patient prognosis. *PLoS One* 2016; 11: e0156274.
- [9] Kim HJ, Eoh KJ, Kim LK, Nam EJ, Yoon SO, Kim KH, Lee JK, Kim SW, Kim YT. The long noncoding RNA HOXA11 antisense induces tumor progression and stemness maintenance in cervical cancer. *Oncotarget* 2016; 7: 83001-83016.
- [10] He Y, Luo Y, Liang B, Ye L, Lu G, He W. Potential applications of MEG3 in cancer diagnosis and prognosis. *Oncotarget* 2017; 8: 73282-73295.
- [11] Bolha L, Ravnik-Glavač M, Glavač D. Long Non-coding RNAs as biomarkers in cancer. *Dis Markers* 2017; 2017: 7243968.
- [12] Barbato S, Solaini G, Fabbri M. MicroRNAs in oncogenesis and tumor suppression. *Int Rev Cell Mol Biol* 2017; 333: 229-268.
- [13] Zhang LG, Zhou XK, Zhou RJ, Lv HZ, Li WP. Long non-coding RNA LINC00673 promotes hepatocellular carcinoma progression and metastasis through negatively regulating miR-205. *Am J Cancer Res* 2017; 7: 2536-2544.
- [14] Cheng Z, Li Z, Ma K, Li X, Tian N, Duan J, Xiao X, Wang Y. Long non-coding RNA XIST promotes glioma tumorigenicity and angiogenesis by acting as a molecular sponge of miR-429. *J Cancer* 2017; 8: 4106-4116.
- [15] Zhang J, Yao T, Wang Y, Yu J, Liu Y, Lin Z. Long noncoding RNA MEG3 is downregulated in cervical cancer and affects cell proliferation and apoptosis by regulating miR-21. *Cancer Biol Ther* 2016; 17: 104-113.
- [16] Li B, Shi C, Zhao J, Li B. Long noncoding RNA CCAT1 functions as a ceRNA to antagonize the effect of miR-410 on the down-regulation of ITPKB in human HCT-116 and HCT-8 cells. *Oncotarget* 2017; 8: 92855-92863.
- [17] Zheng P, Yin Z, Wu Y, Xu Y, Luo Y, Zhang TC. LncRNA HOTAIR promotes cell migration and invasion by regulating MKL1 via inhibition miR206 expression in HeLa cells. *Cell Commun Signal* 2018; 16: 5.
- [18] Helms MW, Kemming D, Contag CH, Pospisil H, Bartkowiak K, Wang A, Chang SY, Buerger H, Brandt BH. TOB1 is regulated by EGF-dependent HER2 and EGFR signaling, is highly phosphorylated, and indicates poor prognosis in node-negative breast cancer. *Cancer Res* 2009; 69: 5049-5056.
- [19] Iwanaga K, Sueoka N, Sato A, Sakuragi T, Sakao Y, Tominaga M, Suzuki T, Yoshida Y, K-Tsuzuku J, Yamamoto T, Hayashi S, Nagasawa K, Sueoka E. Alteration of expression or phosphorylation status of tob, a novel tumor suppressor gene product, is an early event in lung cancer. *Cancer Lett* 2003; 202: 71-79.
- [20] Park GT, Seo EY, Lee KM, Lee DY, Yang JM. Tob is a potential marker gene for the basal layer of the epidermis and is stably expressed in human primary keratinocytes. *Br J Dermatol* 2006; 154: 411-418.
- [21] Kundu J, Wahab SM, Kundu JK, Choi YL, Erkin OC, Lee HS, Park SG, Shin YK. Tob1 induces apoptosis and inhibits proliferation, migration and invasion of gastric cancer cells by activating Smad4 and inhibiting β -catenin signaling. *Int J Oncol* 2012; 41: 839-848.
- [22] Li BS, Zuo QF, Zhao YL, Xiao B, Zhuang Y, Mao XH, Wu C, Yang SM, Zeng H, Zou QM, Guo G. MicroRNA-25 promotes gastric cancer migration, invasion and proliferation by directly targeting transducer of ERBB2, 1 and correlates with poor survival. *Oncogene* 2015; 34: 2556-2565.
- [23] Vrba L, Futscher BW. Epigenetic silencing of MORT is an early event in cancer and is associated with luminal, receptor positive breast tumor subtypes. *J Breast Cancer* 2017; 20: 198-202.
- [24] Dong Z, Zhang A, Liu S, Lu F, Guo Y, Zhang G, Xu F, Shi Y, Shen S, Liang J, Guo W. Aberrant methylation-mediated silencing of lncRNA MEG3 functions as a ceRNA in esophageal cancer. *Mol Cancer Res* 2017; 15: 800-810.
- [25] Yang CM, Wang TH, Chen HC, Li SC, Lee MC, Liou HH, Liu PF, Tseng YK, Shiue YL, Ger LP, Tsai KW. Aberrant DNA hypermethylation-silenced SOX21-AS1 gene expression and its clinical importance in oral cancer. *Clin Epigenetics* 2016; 8: 129.
- [26] Yao J, Deng B, Zheng L, Dou L, Guo Y, Guo K. miR-27b is upregulated in cervical carcinogenesis and promotes cell growth and invasion by regulating CDH11 and epithelial-mesenchymal transition. *Oncol Rep* 2016; 35: 1645-1651.
- [27] Kim HJ, Lee DW, Yim GW, Nam EJ, Kim S, Kim SW, Kim YT. Long non-coding RNA HOTAIR is

TOB1-AS1/miR-27b axis regulates cervical cancer progression

- associated with human cervical cancer progression. *Int J Oncol* 2015; 46: 521-530.
- [28] Zhang Y, Wang T, Huang HQ, Li W, Cheng XL, Yang J. Human MALAT-1 long non-coding RNA is overexpressed in cervical cancer metastasis and promotes cell proliferation, invasion and migration. *J BUON* 2015; 20: 1497-1503.
- [29] Subhash S, Andersson PO, Kosalai ST, Kanduri C, Kanduri M. Global DNA methylation profiling reveals new insights into epigenetically deregulated protein coding and long noncoding RNAs in CLL. *Clin Epigenetics* 2016; 8: 106.
- [30] Liu F, Zhang S, Zhao Z, Mao X, Huang J, Wu Z, Zheng L, Wang Q. MicroRNA-27b up-regulated by human papillomavirus 16 E7 promotes proliferation and suppresses apoptosis by targeting polo-like kinase2 in cervical cancer. *Oncotarget* 2016; 7: 19666-19679.
- [31] Ishteiwy RA, Ward TM, Dykxhoorn DM, Burnstein KL. The microRNA -23b/-27b cluster suppresses the metastatic phenotype of castration-resistant prostate cancer cells. *PLoS One* 2012; 7: e52106.
- [32] Zhu J, Zou Z, Nie P, Kou X, Wu B, Wang S, Song Z, He J. Downregulation of microRNA-27b-3p enhances tamoxifen resistance in breast cancer by increasing NR5A2 and CREB1 expression. *Cell Death Dis* 2016; 7: e2454.
- [33] Wang Y, Zhang W, Wang Y, Wang S. HOXD-AS1 promotes cell proliferation, migration and invasion through miR-608/FZD4 axis in ovarian cancer. *Am J Cancer Res* 2018; 8: 170-182.
- [34] Wen Q, Liu Y, Lyu H, Xu X, Wu Q, Liu N, Yin Q, Li J, Sheng X. Long Noncoding RNA GAS5, which acts as a tumor suppressor via microRNA 21, regulates cisplatin resistance expression in cervical cancer. *Int J Gynecol Cancer* 2017; 27: 1096-1108.
- [35] Jin X, Chen X, Hu Y, Ying F, Zou R, Lin F, Shi Z, Zhu X, Yan X, Li S, Zhu H. LncRNA-TCO-NS_00026907 is involved in the progression and prognosis of cervical cancer through inhibiting miR-143-5p. *Cancer Med* 2017; 6: 1409-1423.
- [36] Fang Q, Chen X, Zhi X. Long non-coding RNA (LncRNA) urothelial carcinoma associated 1 (UCA1) increases multi-drug resistance of gastric cancer via downregulating miR-27b. *Med Sci Monit* 2016; 22: 3506-3513.
- [37] Wu X, Yan T, Wang Z, Wu X, Cao G, Zhang C. LncRNA ZEB2-AS1 promotes bladder cancer cell proliferation and inhibits apoptosis by regulating miR-27b. *Biomed Pharmacother* 2017; 96: 299-304.